arXiv:cond-mat/0407702v2 [cond-mat.stat-mech] 20 Jan 2005

Quantum ratchets in dissipative chaotic systems

Gabriel G. Carlo,[1] Giuliano Benenti,[1] Giulio Casati,[1] and Dima L. Shepelyansky[2]

[1]*Center for Nonlinear and Complex Systems, Università degli Studi dell'Insubria and Istituto Nazionale per la Fisica della Materia, Unità di Como, Via Valleggio 11, 22100 Como, Italy*

[2]*Laboratoire de Physique Théorique, UMR 5152 du CNRS, Université Paul Sabatier, 31062 Touluse Cedex 4, France*

(Dated: July 27, 2004; Revised: January 19, 2005)

Using the method of quantum trajectories we study a quantum chaotic dissipative ratchet appearing for particles in a pulsed asymmetric potential in the presence of a dissipative environment. The system is characterized by directed transport emerging from a quantum strange attractor. This model exhibits, in the limit of small effective Planck constant, a transition from quantum to classical behavior, in agreement with the correspondence principle. We also discuss parameter values suitable for implementation of the quantum ratchet effect with cold atoms in optical lattices.

PACS numbers: 05.45.Mt, 05.40.Jc, 05.60.-k, 32.80.Pj

Cold atoms exposed to time-dependent standing waves of light provide an ideal test bed to explore the features of the quantum dynamics of nonlinear systems. They allowed the experimental investigation of several important physical phenomena, such as dynamical localization [1, 2], decoherence [3], quantum resonances [4], and chaos assisted tunneling [5, 6]. In particular, they made possible to realize experimentally the quantum kicked rotor [1, 2, 3, 4], a paradigmatic model in the field of quantum chaos [7]. Furthermore, cold atoms in optical lattices allowed to demonstrate the ratchet phenomenon [8, 9, 10], that is characterized by directed transport in the absence of any net force.

Directed transport [11, 12] is found in periodic systems due to a broken spatial-temporal symmetry [13], for instance in presence of lattice asymmetry, unbiased periodic driving and dissipation. This phenomenon, also called ratchet effect, is of potential relevance in technological applications such as rectifiers, pumps, particle separation devices, molecular switches, and transistors. Moreover, it is of great interest for the understanding of molecular motors in biology [14]. In previous works, attention has been focused on systems with external noise, on chaotic dynamical systems with dissipation and on purely Hamiltonian systems (with mixed or chaotic phase space) [15, 16, 17, 18, 19, 20, 21]. In particular, the issue of current reversal has attracted much interest [22, 23, 24, 25]. It was found that current reversal can be originated by a bifurcation from a chaotic to a periodic regime, that is, by the transition from a strange attractor to a simple one [23].

The presence of strange attractors is a characteristic feature of classical dissipative chaotic systems [26]. In quantum mechanics, it was found that the fractal structure of the classical strange attractor is smoothed on the scale of Planck's cell [27]. It is therefore interesting to investigate how this phenomenon affects quantum ratchets. Till present the effects of dissipation have been mainly analyzed for classical ratchets while for quantum motion the theoretical studies have been concentrated on the Hamiltonian case [17, 18, 19]. In this Letter, we study a quantum ratchet system which is in contact with a dissipative environment and whose classical counterpart is chaotic. The investigation is carried out for parameter values where a strange attractor is present. Using the quantum trajectories approach, we are able to simulate numerically the evolution of a fractal quantum ratchet emerging from a quantum strange attractor. Moreover, we show that the ratchet effect is robust in presence of noise. Finally, we consider parameter values which should allow the observation of quantum chaotic dissipative ratchets in cold atoms experiments.

We study a particle moving in one dimension [$x \in (-\infty, +\infty)$] in a periodic kicked asymmetric potential:

$$V(x,\tau) = k\left[\cos(x) + \frac{a}{2}\cos(2x+\phi)\right] \sum_{m=-\infty}^{+\infty} \delta(\tau - mT), \tag{1}$$

where T is the kicking period. The evolution of the system in one period is described by the map

$$\begin{cases} \overline{n} = \gamma n + k(\sin(x) + a\sin(2x+\phi)), \\ \overline{x} = x + T\overline{n}, \end{cases} \tag{2}$$

where n is the momentum variable conjugated to x and γ is the dissipation parameter, describing a velocity proportional damping. We have $0 \leq \gamma \leq 1$; the limiting cases $\gamma = 0$ and $\gamma = 1$ correspond to overdamping and Hamiltonian evolution, respectively. Introducing the rescaled momentum variable $p = Tn$, one can see that classical dynamics depends on the parameter $K = kT$ (not on k and T separately). We note that at $a = 0$ the classical model reduces to the Zaslavsky map [29]. However, due to the symmetry of the potential, the ratchet effect is absent in this case (see discussion below). The quantum model is obtained by means of the usual quantization rules [7]: $x \to \hat{x}$, $n \to \hat{n} = -i(d/dx)$ (we set

$\hbar = 1$). Since $[\hat{x}, \hat{p}] = iT$, the effective Planck constant is $\hbar_{\rm eff} = T$. The classical limit corresponds to $\hbar_{\rm eff} \to 0$, while keeping $K = \hbar_{\rm eff} k$ constant.

In order to simulate a dissipative environment in the quantum model we consider a master equation in the Lindblad form [28] for the density operator $\hat{\rho}$ of the system. We have

$$\dot{\hat{\rho}} = -i[\hat{H}_s, \hat{\rho}] - \frac{1}{2}\sum_{\mu=1}^{2}\{\hat{L}_\mu^\dagger \hat{L}_\mu, \hat{\rho}\} + \sum_{\mu=1}^{2}\hat{L}_\mu \hat{\rho}\hat{L}_\mu^\dagger, \qquad (3)$$

where $\hat{H}_s = \hat{n}^2/2 + V(\hat{x}, \tau)$ is the system Hamiltonian, $\hat{L}_\mu$ are the Lindblad operators, and $\{\,,\}$ denotes the anticommutator. We assume that dissipation is described by the lowering operators

$$\begin{array}{l} \hat{L}_1 = g\sum_n \sqrt{n+1}\,|n\rangle\langle n+1|, \\ \hat{L}_2 = g\sum_n \sqrt{n+1}\,|-n\rangle\langle -n-1|, \end{array} \qquad (4)$$

with $n = 0, 1, ...$ [30]. Requiring that at short times $\langle p\rangle$ evolves like in the classical case, as it should be according to the Ehrenfest theorem, we obtain $g = \sqrt{-\ln\gamma}$.

The first two terms of Eq. (3) can be regarded as the evolution governed by an effective non-Hermitian Hamiltonian, $\hat{H}_{\rm eff} = \hat{H}_s + i\hat{W}$, with $\hat{W} = -1/2\sum_\mu \hat{L}_\mu^\dagger \hat{L}_\mu$. In turn, the last term is responsible for the so-called quantum jumps. Taking an initial pure state $|\phi(\tau_0)\rangle$, the jump probabilities dp_μ in an infinitesimal time $d\tau$ are defined by $dp_\mu = \langle\phi(\tau_0)|\hat{L}_\mu^\dagger \hat{L}_\mu|\phi(\tau_0)\rangle d\tau$, and the new states after the jumps by $|\phi_\mu\rangle = \hat{L}_\mu|\phi(\tau_0)\rangle/||\hat{L}_\mu|\phi(\tau_0)\rangle||$. With probability dp_μ a jump occurs and the system is left in the state $|\phi_\mu\rangle$. With probability $1 - \sum_\mu dp_\mu$ there are no jumps and the system evolves according to the effective Hamiltonian $\hat{H}_{\rm eff}$. In order to simulate the master equation (3), we have used the quantum trajectories approach [31]. We start from a pure state $|\phi(\tau_0)\rangle$ and, at intervals $d\tau$, we perform the following evaluation. We choose a random number ϵ from a uniform distribution in the unit interval $[0, 1]$. If $\epsilon < dp$, where $dp = \sum_{\mu=1}^{2} dp_\mu$, the system jumps to one of the states $|\phi_\mu\rangle$ (to $|\phi_1\rangle$ if $0 \le \epsilon \le dp_1$ or to $|\phi_2\rangle$ if $dp_1 < \epsilon \le dp_1 + dp_2$). On the other hand, if $\epsilon > dp$, the evolution with the non-Hermitian Hamiltonian $\hat{H}_{\rm eff}$ takes place, ending up in a state that we call $|\phi_0\rangle$. In both circumstances we renormalize the state. We repeat this process as many times as $n_{\rm steps} = (\Delta\tau)/d\tau$ where $\Delta\tau$ is the whole elapsed time during the evolution. Note that we must take $d\tau$ much smaller than the time scales relevant for the evolution of the open quantum system under investigation. In our simulations, $d\tau$ is inversely proportional to $\hbar_{\rm eff}$. Given any observable A, we can write the mean value $\langle A\rangle_\tau = {\rm Tr}[\hat{A}\hat{\rho}(\tau)]$ as the average over $\mathcal{N}$ trajectories:

$$\langle A\rangle_\tau = \lim_{\mathcal{N}\to\infty}\frac{1}{\mathcal{N}}\sum_{i=1}^{\mathcal{N}}\langle\phi_i(\tau)|\hat{A}|\phi_i(\tau)\rangle. \qquad (5)$$

We found that a reasonable amount of trajectories ($\mathcal{N} \simeq 100 - 500$) is sufficient in order to obtain a satisfactory statistical convergence. We used up to 3^8 quantum levels to investigate the transition from quantum to classical behavior.

The appearance of a strange attractor in our model is shown in the phase space portraits of Fig. 1, for parameter values $K = 7$, $\gamma = 0.7$, $\phi = \pi/2$, $a = 0.7$ [32]. The left panel (classical mechanics) corresponds to a Poincare section constructed from 10^7 random initial conditions uniformly distributed in the area $x \in [0, 2\pi)$, $p \in [-\pi; \pi]$, after 100 iterations of map (2). From top to bottom we zoom in, showing the fractal structure of the attractor down to smaller and smaller scales. On the right column (quantum mechanics, $\hbar_{\rm eff} = 0.012$) we show the corresponding Husimi functions [33] averaged over $N_i = 5$ initial conditions (randomly selected p values in the same interval as before), considering $\mathcal{N} = 160$ trajectories for each initial condition. We can see a good agreement between the classical and the quantum phase space portraits. Though the quantum version is less detailed the main classical patterns are well reproduced. On the other hand, a magnification of a small part of the phase space shows that the resolution of the quantum picture is limited by the uncertainty principle.

The attractor in Fig. 1 is strongly asymmetric, suggesting directed transport, that is, $\langle p\rangle \neq 0$. This is confirmed by the numerical data of Fig. 2, where $\langle p\rangle$ is shown as a function of time, both in the classical and in the quantum case (for $\hbar_{\rm eff} = 0.037, 0.11, 0.33, 0.99$). In the classical case, $\langle p\rangle$ saturates after a very short time scale (approximately 10 kicks) required for the setting in of the strange attractor. In the quantum case, a gradual approach to the classical limit can be clearly seen as $\hbar_{\rm eff}$ is reduced, in agreement with the correspondence principle The difference $\delta\langle p\rangle$ between the classical and quantum saturation currents is shown as a function of $\hbar_{\rm eff}$ in the inset of Fig. 2. In the same inset, we also show the numerical fit $\delta\langle p\rangle \propto \hbar_{\rm eff}^\nu$, with the fitting constant $\nu \approx 0.6$. We see that the quantum fluctuations lead to a smaller value of the directed current as compared to the classical case.

In Fig. 3, we show that it is possible to control the direction of transport by varying the phase ϕ. We observe that $\langle p\rangle_{-\phi} = -\langle p\rangle_\phi$. This is due to the fact that the potential $V(x, \tau)$ has the symmetry $V_\phi(x, \tau) = V_{-\phi}(-x, \tau)$. Therefore, the current can be reversed by changing $\phi \to -\phi$. In particular, there is a space symmetry for $\phi = n\pi$ [in these cases, $V(x, \tau) = V(-x, \tau)$], which implies zero net current. This is confirmed, at $\phi = 0$, from the numerical data of Fig. 3.

We point out that quantum directed transport is observed in our model also for parameter values where the classical dynamics is characterized by a simple attractor (fixed points) instead of a strange one. Moreover, we have explored a different dissipation mechanism (*i.e.*, loss of probability for $|p|$ larger than some threshold value $p_{\rm th}$

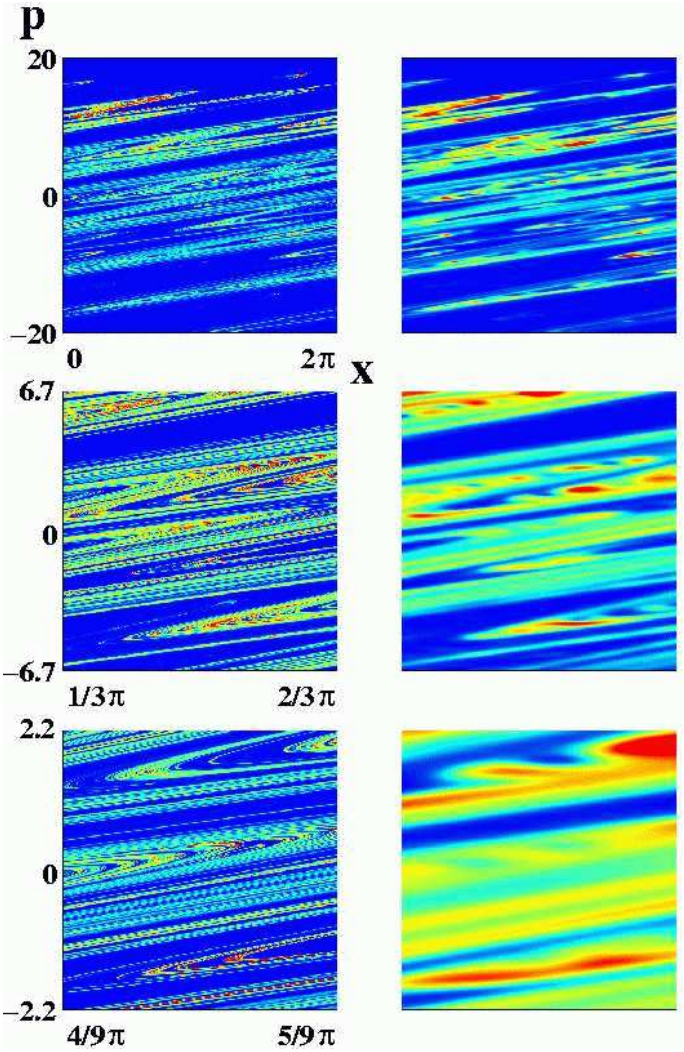


FIG. 1: (Color) Phase space pictures for $K = 7$, $\gamma = 0.7$, $\phi = \pi/2$, $a = 0.7$, after 100 kicks: classical Poincaré sections (left) and quantum Husimi functions at $\hbar_{\rm eff} = 0.012$ (right). In the upper row, the displayed region is given by $p \in [-20, 20]$ and $x \in [0, 2\pi)$ (note that, to draw the attractor, x is taken modulus 2π). Magnifications of these plots are shown in the second and third rows (the area is reduced by a factor 1/9 and 1/81, respectively). The color is proportional to the density: blue for zero and red for maximal density.

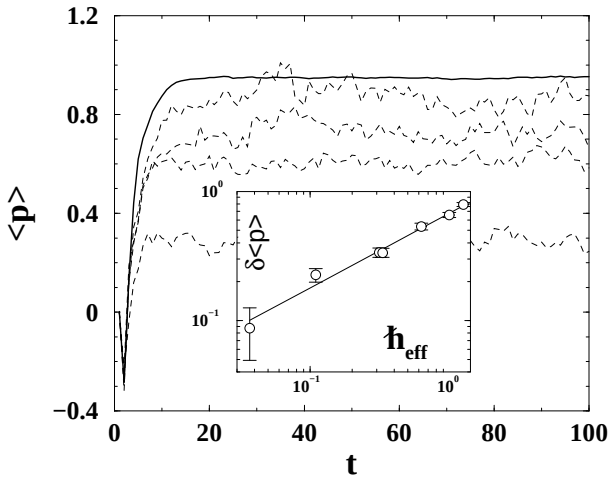


FIG. 2: Average momentum $\langle p \rangle$ as a function of time t (measured in number of kicks), with same parameter values as in Fig. 1. The solid curve corresponds to the classical limit, while the other curves are quantum results at (from bottom to top) $\hbar_{\rm eff} = 0.99, 0.33, 0.11, 0.037$. Each quantum curve is obtained from $N_i = 60$ initial conditions and $\mathcal{N} = 480$ trajectories for each initial conditions. Inset: scaling of $\delta\langle p \rangle$ with $\hbar_{\rm eff}$ (circles). The power-law fit $\delta\langle p \rangle \propto \hbar_{\rm eff}^{\nu}$ gives $\nu \approx 0.6$ (full line).

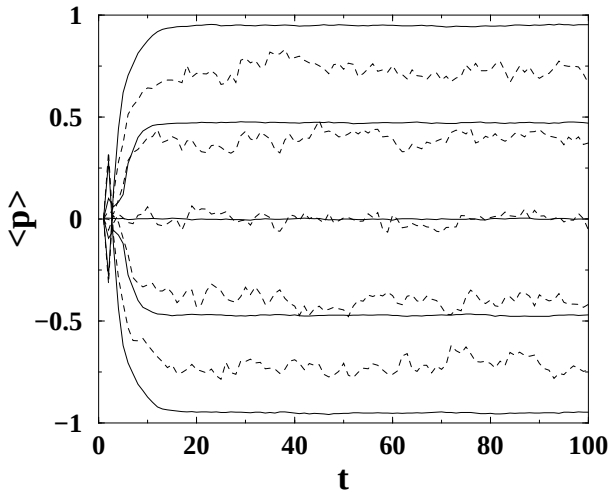


FIG. 3: Average momentum versus time, for (from top to bottom) $\phi = \pi/2, 2\pi/5, 0, -2\pi/5, -\pi/2$, in the classical (full curves) and in the quantum case (dashed curves, $\hbar_{\rm eff} = 0.11$). The other parameter values are as in Figs. 1 and 2.

after each kick [34]) and found that this case is also characterized by directed transport and a quantum strange repeller [35]. This is a further demonstration that quantum ratchets and asymmetric strange attractors and repellers are a typical feature of open quantum systems which are chaotic in the classical limit.

It is important to analyze the stability of our ratchet phenomenon in respect to noise effects. For this purpose, we introduce memoryless fluctuations in the kicking strength: $K \to K_\epsilon(t) = K + \epsilon(t)$, where the noise values $\epsilon(t)$ are uniformly and randomly distributed in the interval $[-\epsilon, +\epsilon]$. The dependence of the classical and quantum currents on ϵ is shown in Fig. 4. We can see that directed transport survives, both in the classical and in the quantum case, up to a noise strength ϵ of the order of the kicking strength K. We stress that the robustness of our ratchet model is in contrasts with the behavior of the quantum Hamiltonian ratchets discussed in Refs. [17, 18]. Indeed, noise eliminates the ratchet ef-

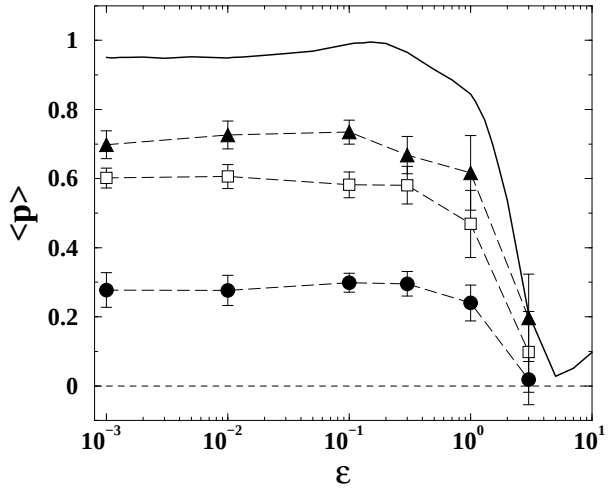


FIG. 4: Average momentum versus noise strength, in the classical (full curve) and in the quantum case, for $\hbar_{\rm eff} = 0.99$ (circles), 0.33 (squares), and 0.11 (triangles). The other parameter values are as in Figs. 1,2.

fect in Hamiltonian systems at large time scales, while in our case the ratchet is produced by dissipation and remains stable with respect to introduction of noise. We also note that the reduction of ratchet current with noise (Fig. 4) gives a qualitative reason for reduction of the current with increase of $\hbar_{eff}$ (Fig. 2) which leads to growth of quantum fluctuations.

The model discussed here can be realized experimentally with cold atoms in a periodic standing wave of light, with parameters similar to those of Refs. [1, 2, 3, 4, 5]. For example, it is possible to use sodium atoms in a laser field with wave length $\lambda_L = 589$ nm [1], which creates effective pulsed potential with classical chaos parameter $K = \sqrt{2\pi}\alpha\Omega_{\rm eff}\omega_r T^2$ and $\hbar_{\rm eff} = 8\omega_r T$. Here T is the pulse periodicity, $\Omega_{\rm eff}$ the effective Rabi frequency, $\omega_r = \hbar k_L^2/2M$ the recoil frequency ($k_L = 1/\lambda_L$, M atomic mass) and α is the fraction of Gaussian pulse duration in units of pulse period. For typical parameter conditions of Ref. [1], it is possible to take $\Omega_{\rm eff}/2\pi = 75$ MHz, $T = 0.8$ μs, $\alpha = 0.05$, which gives $\hbar_{\rm eff} \approx 1$, $K \approx 5$, being similar to the case of Fig.2 [36]. A dissipative friction force can be created by additional laser fields which for sodium atoms can easily produce a dissipation rate $2\beta \approx 4 \times 10^5$ s^{-1} [37] giving $1 - \gamma = 2\beta T \approx 0.3$. We also note that the Husimi function can in principle be measured from a state reconstruction technique [38]. This could allow the experimental observation of a quantum strange ratchet attractor.

We acknowledge fruitful discussions with Marcos Saraceno. This work was supported in part by EU (IST-FET-EDIQIP) and NSA-ARDA (ARO contract No. DAAD19-02-1-0086).

[1] F.L. Moore *et al.*, Phys. Rev. Lett. **75**, 4598 (1995).
[2] J. Ringot *et al.*, Phys. Rev. Lett. **85**, 2741 (2000).
[3] H. Ammann *et al.*, Phys. Rev. Lett. **80**, 4111 (1998).
[4] M.B. d'Arcy *et al.*, Phys. Rev. Lett. **87**, 074102 (2001).
[5] D.A. Steck *et al.*, Science **293**, 274 (2001).
[6] W.K. Hensinger *et al.*, Nature **412**, 52 (2001).
[7] G. Casati and B. Chirikov (Eds.), *Quantum Chaos: Between Order and Disorder*, Cambridge Univ. Press (1995); F.M.Izrailev, Phys. Rep. **196**, 299 (1990).
[8] C. Mennerat-Robilliard *et al.*, Phys. Rev. Lett. **82**, 851 (1999).
[9] M. Schiavoni *et al.*, Phys. Rev. Lett. **90**, 094101 (2003).
[10] P.H. Jones *et al.*, quant-ph/0309149.
[11] R.D. Astumian and P. Hänggi, Physics Today **55** (11), 33 (2002).
[12] P. Reimann, Phys. Rep. **361**, 57 (2002).
[13] S. Flach *et al.*, Phys. Rev. Lett. **84**, 2358 (2000).
[14] F. Jülicher *et al.*, Rev. Mod. Phys. **69**, 1269 (1997).
[15] P. Jung *et al.*, Phys. Rev. Lett. **76**, 3436 (1996).
[16] M. Porto *et al.*, Phys. Rev. Lett. **85**, 491 (2000).
[17] H. Schanz *et al.*, Phys. Rev. Lett. **87**, 070601 (2001); L. Hufnagel *et al.*, *ibid.* **89**, 154101 (2002).
[18] T.S. Monteiro *et al.*, Phys. Rev. Lett. **89**, 194102 (2002).
[19] T. Jonckheere *et al.*, Phys. Rev. Lett. **91**, 253003 (2003).
[20] T. Cheon *et al.*, J. Phys. Soc. Jpn. **72**, 1087 (2003).
[21] J. Gong and P. Brumer, Phys. Rev. E **70**, 016202 (2004).
[22] R. Bartussek *et al.*, Europhys. Lett. **28**, 459 (1994).
[23] J.L. Mateos, Phys. Rev. Lett. **84**, 258 (2000).
[24] M. Barbi and M. Salerno, Phys. Rev. E **62**, 1988 (2000).
[25] D. Dan *et al.*, Phys. Rev. E **63**, 056307 (2001).
[26] E. Ott, *Chaos in dynamical systems*, Cambridge Univ. Press (1993).
[27] T. Dittrich and R. Graham, Annals of Physics **200**, 363 (1990).
[28] G. Lindblad, Commun. Math. Phys. **48**, 119 (1976); V. Gorini *et al.*, J. Math. Phys. **17**, 821 (1976).
[29] R.Z. Sagdeev *et al.*, *Nonlinear Physics*, Harwood Acad. Pub., NY (1988).
[30] These Lindblad operators can be obtained, similarly to [27], by considering the interaction between the system and a bosonic bath. The master equation (3) is then derived, at zero temperature, in the usual weak coupling and Markov approximations.
[31] J. Dalibard *et al.*, Phys. Rev. Lett. **68**, 580 (1992).
[32] There are also other similar parameter values where the system exhibits a simple or chaotic attractor.
[33] The Husimi function is obtained from smoothing of the Wigner function on a scale of Planck constant, see e.g. S.-J. Chang and K.-J. Shi, Phys. Rev. A **34**, 7 (1986).
[34] G.Casati *et al.*, Physica D **131**, 311 (1999).
[35] That is to say, a repelling chaotic limit set.
[36] At $\hbar_{\rm eff} \approx 1$ the ratchet current is $\langle p \rangle/\hbar_{\rm eff} \approx 0.3$ (see Fig.2), that corresponds to momentum equal to 0.3, expressed in units of double photon recoil, $2\hbar k_L$. This is significantly larger than the experimental resolution equal to 0.03 [5].
[37] E.L. Raab *et al.*, Phys. Rev. Lett. **59**, 2631 (1987).
[38] M. Bienert *et al.*, Phys. Rev. Lett. **89**, 050403 (2002).